NUMERICAL STUDY ON THERMAL PERFORMANCE OF WATER FLOW IN A TWISTED DUCT HEAT EXCHANGER

Musaab K. RASHED[*], Kadhum Audaa JEHHEF, Faris Ali BADAWY
Middle Technical University, Institute of Technology, Baghdad/ Iraq.
E-mail: musaabk.rasheed@mtu.edu.iq

This paper presents a numerical study of heat transfer through a downstream annulus using water as the working fluid within the laminar flow region. The annulus consisted of an outer twisted square duct and an inner circular pipe. A three-dimensional formulation was used to solve the Navier-Stokes equations numerically for the laminar flow system with a low Reynolds number. Three parameters were used in the numerical simulation: the length of the twisted square $(a: 6.6, 8.2\ 10.2, 12.6\ mm)$; the inner diameter of the inner circular pipe $(d: 19, 21, 23\ and\ 25\ mm)$; and the twist angle $(\theta: 0^o\ (\text{smooth}), 45^o, 60^o\ and\ 90^o)$. Numerical calculations were conducted on sixteen twisted square duct heat exchangers, with water flowing within a Reynolds number range of $220-1100$. The results were illustrated as a profile of the thermal enhancement factor, the friction factor and the Nusselt number. The results show that the twisted outer duct of the heat exchanger can create a swirl flow along the length of the heat exchanger. It also caused a boundary layer separation-reattachment on the wall of the inner pipe. Moreover, an increase in the twist angle increased the Nusselt number by $20\ \%$, and the friction factor was also increased as the annular gap of the heat exchanger decreased.

Keywords: mixed convection, twisted square duct, heat exchanger, laminar flow.

1. Introduction

Passive techniques that are used to improve the heat transfer efficiency of heat exchangers vary according to different applications. There are many methods and types of passive techniques that are employed in thermal applications including rough surfaces, displaced promoters, vortex devices and extended surfaces. Many of these techniques require an addition of some external materials to the original configuration of the system (as is the case with displaced promoters, vortex devices and extended surfaces), which increases the cost of the thermal system. In other techniques, such as twisted pipes, dimple pipes and corrugated pipes, it is not necessary to add any materials. The main purpose is to enhance the heat transfer from the flow in the inner tube to the flow in the annulus and vice versa by increasing the heat transfer coefficient in the inner tube or in the annulus.

Vyver and Meyer [1] considered a simple heat exchanger that includes an aluminum circular tube inside a twisted square tube with a length of *3* m. They showed that both the Nusselt number and the friction factor of the annulus increase with an increase in the twist angle of the twisted square tube and the Reynolds number. The maximum Nusselt number was found at a 105° twist angle and when *Re = 14000.* Timité *et al.* [2] investigated both experimentally and numerically the mixing flow and heat transfer enhancement in a twisted curved-pipe. Their results showed that the tracer pattern increases in relation to the distance along the twisted pipe with a pulsating flow in the same manner as in a steady chaotic twisted-pipe flow. Bhattacharyya *et al.* [3] modeled the fluid flow and heat transfer of air flow in an elliptical twisted duct with Reynolds numbers ranging from $1000-3500$. The pitch length ranged between *0.5* and *1.0*, while the aspect ratio of the elliptical duct was 0.5. They found that the Nusselt enhancement Nu/Nu$_0$ increased from

---

[*] To whom correspondence should be addressed

1.14 to *1.23* when the pitch length (Y) was decreased from *0.62* to *0.5*. Castelain *et al.* [4] studied the three-dimensional laminar flow in a twisted duct with four 90° bends. The centrifugal forces produced due to the change in the curvature plane of the flow generated the Dean roll-cells, which are the source of the fluid particles irregular trajectories. Their results showed that the maximum peak of axial velocity increased with an increase in the Dean numbers. Eiamsa-ard and Changcharoen [5] presented a numerical simulation to predict the characteristics of an incompressible air periodic flow in square ducts with dual and quadruple twisted tapes with different configurations. Their results revealed that the maximum Nusselt number was obtained when using quadruple counter tapes (CC-QTs), but also that the model of quadruple counter-tapes (PC-QTs) gave the maximum friction factor when compared to the smooth duct. Patil and Vijay [6] experimentally investigated the ethylene glycol laminar flow in a square duct fitted with twisted tapes to predict the characteristics of heat transfer and friction factor for different twists. The Nusselt numbers were found to be between *5.44* and *7.49* times more than that of plain, square duct forced convection values. Promvonge *et al.* [7] studied the effect of using twisted-tape and winglet vortex generators on the heat transfer enhancement of the airflow inside a square duct. The features of the twisted-tape using different twist ratios, winglet to duct-height ratios, winglet-pitch to tape-width ratios, and attack angle were reported. Promvonge [8] presented an experimental study to investigate the influence of the fin height, fin pitch and attack angle on the fluid flow and heat transfer enhancement in a square duct with V-fins and quadruple counter-twisted tapes. Promvonge's results revealed that when using V-finned counter-twisted tapes, the Nusselt numbers and the friction factor were increased with an increase in the fin height (R_B) and a decrease in the fin pitch (R_P). The maximum Nusselt numbers were found at the largest R_B but at the smallest R_P. Rashid *et al.* [9] conducted a 3D numerical thermo-hydrodynamic and a second flow analysis of the flow of a nanofluid within a square conduit outfitted with transverse-twisted baffles. The impacts of changes in the pitch ratio (γ) from *180* to *540* and in the volume of nanoparticles (φ) from *0* to *0.05* on the nanofluid heat convection and thermodynamics were examined. The numerical findings showed that the highest heat transfer coefficient was obtained for a baffle with a pitch value of $\gamma = 360^o$. Yang *et al.* [10] investigated the thermal performance and water flow resistance characteristics within twisted elliptical tubes (TETs) with various structural factors. They analyzed the impacts of twist pitch and aspect ratio on the efficiency of TETs, and they also evaluated the overall thermal-hydraulic efficiency of TETs. High friction factors and heat transfer coefficients were demonstrated with large tube aspect ratios and small twist pitches. The best performance of TETs was seen at lower Reynolds numbers. Zhang *et al.* [11] experimentally explored the heat transfer rate attributes of steam condensation on horizontally twisted elliptical tubes (TETs) with various structural configurations. The condensation heat transfer coefficients were reduced by increasing the wall sub-cooling. The results also showed that not all the examined TETs had better condensation heat transfer performance than the smooth circular tube (the normal improvement factors given by the five TETs ranged from *0.87* to *1.34*). K.A. Jehhef *et al.* [12] investigated the mixed convection between two parallel plates of a vertical channel in the presence of a triangular rib. The contribution of forced and free convection to the total heat transfer was also analyzed. The results showed that the Nusselt number and the friction factor increased when using the attached triangular ribs, particularly with respect to the downstream ribs.

This paper explores the possibility of uncomplicated and inexpensive methods of heat transfer amplification that could be utilized by small manufacturing organizations. The heat exchanger considered here is like a tube-in-tube heat exchanger, with an inner round tube and an outer square twisted duct. The aim, in this case, is to build the movement of heat in the annulus using swirl water flow. The force of the swirl movement is influenced by a part of the outer square duct.

2. Problem formulation

The computational domain of the circular double pipe heat exchanger, consisting of a circular inner pipe and square outer twisted pipe, is represented in a two-dimensional (2D) form and is shown in Fig.1. The

geometry consists of a circular inner pipe with an inner diameter of (d) and square outer twisted duct with a side length of (a) and twisted angle of (θ). The overall heat exchanger length is fixed at (L).
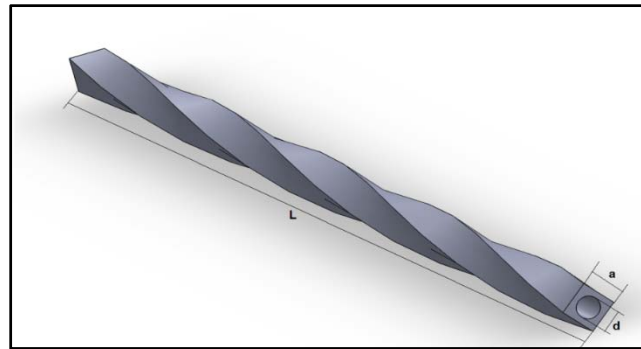
Fig.1. Geometry schematic of the twisted double pipe heat exchanger given by Solidworks v.2018.

In this work, a numerical analysis of the mixed convection of the water flow and heat transfer in the twisted heat exchanger was conducted. The main purpose of this work was to determine the boundaries of the operating and geometric parameters, as set out in Tab.1, at which a transition of the prevalent influence of mixed convection is noticed. An additional aim was to identify the effects of twist on the heat transfer mechanisms when changing the geometry from a smooth to a twisted annulus in the double heat exchanger.

Table1. Operating and geometry parameters employed in this study.

Reynolds number Re	Duct wall side a (mm)	Pipe diameter (d) mm	Twisted Angle θ (º)
220	19	6.6	0
440	21	8.6	45
660	23	10.6	60
1100	25	12.6	90
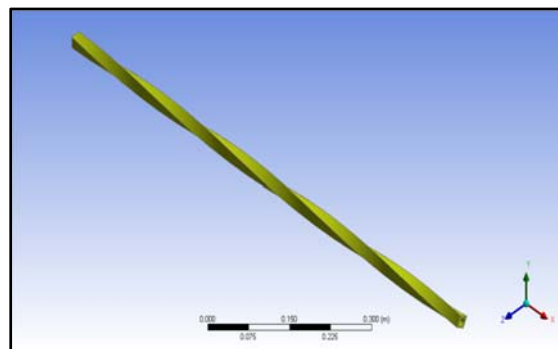
Fig.2. Schematic geometry of twisted double pipe heat exchanger given by Design Modular v.12.

The shape of the double pipe heat exchanger is shown in Fig.2. The heat exchanger was fixed at $(L = 1200 \; mm)$, but four models for the ratio of the duct side length to the inner pipe diameter (a / d) and twisted angle (θ) were considered. The twisted duct walls were supposed to be thermally insulated and the

inner pipe was kept at a fixed heat flux q. In the annular region between the twisted duct and the inner pipe, the forced water flow rate and its temperature are constant and equal to both u_o and T_o, respectively.

2.1. Mathematical model

The mathematical model for the problem used two-dimensional Navier-Stokes equations, and it was assumed that the laminar heat transfer need not be taken into account; however, the influence of gravity was considered using the Boussines q approximation. The main fluid was water, with a Prandtl number $(\text{Pr}) = 1.7$. Note that the problem was resolved by two dimensionless values, Richardson and Reynolds, which characterize the effect of mixed convection. In the present work, the Reynolds number ranged as follows:

$$\text{Re} = \frac{u_o D_h}{v} = 220,440,660 \quad \text{and} \quad 1100 . \tag{2.1}$$

The hydraulic diameter D_h depends on the volume of the annulus divided by the heat exchanger length and circumference, which is given by:

$$D_h = \frac{4.V_a}{A_s} . \tag{2.2}$$

A_s is the heated surface area and is calculated by:

$$A_s = \pi dL . \tag{2.3}$$

The volume available for the flow of fluid in the annulus, V_a, can be determined by knowing the geometrical dimensions of the twisted heat exchanger, and it can be written as:

$$V_a = \left(a^2 - \frac{\pi}{4} d^2 \right) L . \tag{2.4}$$

The single-phase model equations involve the equations for continuity, momentum and energy for the ANSYS Fluent 16.2. The equations of continuity and momentum are utilized to determine the velocity vector field, while the energy equation is calculated from the temperature distribution and wall heat transfer coefficient. The equation for conservation of mass, or the continuity equation, can be written as follows:

Mass Conservation Equation

The continuity equation is written as:

$$\frac{\partial \rho}{\partial t} + \nabla . (\rho \vec{v}) = S_m . \tag{2.5}$$

Equation (2.5) is valid for both an incompressible and compressible fluid flow. S_m is the source that represents the mass added to the continuous phase from the dispersed second phase (e.g., due to vaporization of liquid droplets) and any user-defined sources. It is neglected in the present case.

Momentum Conservation Equation

The conservation of momentum in an inertial (non-accelerating) reference frame is described by:

$$\frac{\partial}{\partial t}(\rho \vec{v}) + \nabla \cdot (\rho \vec{v} \vec{v}) = -\nabla p + \nabla \cdot \left(\overline{\overline{\tau}} \right) + \rho \vec{g} + \vec{F} \tag{2.6}$$

where p is the static pressure, $\overline{\overline{\tau}}$ is the stress tensor, $\rho \vec{g}$ is the gravitational body force, and $\vec{F}$ is the external body force (e.g., that arises from interaction with the dispersed phase), and it is neglected in the present case. $\vec{F}$ also contains other model dependent source terms such as porous-media and user-defined sources. The stress tensor $\overline{\overline{\tau}}$ is given by:

$$\overline{\overline{\tau}} = \mu \left[\left(\nabla \vec{v} + \nabla \vec{v}^T \right) - \frac{2}{3} \nabla \cdot \vec{v} I \right] \tag{2.7}$$

where μ is the molecular viscosity, I is the unit tensor, and the second term on the right hand side is the effect of volume dilation.

Energy equation

In the ANSYS FLUENT solver, the energy equation is used to predict the temperature distribution in the computational domain, and it is written as:

$$\frac{\partial}{\partial t}(\rho E) + \nabla \cdot (\vec{v}(\rho E + p)) = \nabla \cdot \left[k_{eff} \nabla T - \sum_j h_j J_j + \left(\overline{\overline{\tau}}_{eff} \cdot \vec{v} \right) \right] + S_h \tag{2.8}$$

where K_{eff} represents the effective conductivity, which consists of $(\kappa + \kappa_t)$, where κ_t is the turbulent thermal conductivity that is defined according to the turbulence model being used, and $\overline{J}_j$ represents the diffusion flux of species J. The first three terms on the right-hand side of Eq. (2.8) represent the energy transfer due to conduction, species diffusion, and viscous dissipation, respectively. S_h contains the heat of the chemical reaction, and any other volumetric heat sources, and it is neglected in the present case. The E term can be written as:

$$E = h - \frac{p}{\rho} + \frac{v^2}{2} \tag{2.9}$$

Sensible enthalpy, h, is well-defined for ideal gases as:

$$h = \sum_j Y_j h_j \tag{2.10}$$

Y_j is the mass fraction of species, where j is defined as:

$$h_j = \int_{T_{ref}}^{T} c_{p,j} \, dT \tag{2.11}$$

T_f is used as *298.15 K*.

The skin friction coefficient, C_f, is given by:

$$C_f = 2\tau_w / \rho \bar{U}^2. \tag{2.12}$$

The friction factor, f, is calculated as:

$$f = 2\left(\frac{\Delta P}{L}\right) D_h / \rho \bar{U}^2. \tag{2.13}$$

The local Nusselt number, Nu_x, can be written as:

$$Nu_x = h_x D_h / k_f. \tag{2.14}$$

The average Nusselt number, Nu, can be obtained by:

$$Nu = \frac{1}{H} \int_0^L Nu_x \, dx. \tag{2.15}$$

The following expression represents the Thermal Enhancement Factor, TEF:

$$TEF = \left(Nu / Nu_o\right) / \left(f / f_o\right)^{1/3}. \tag{2.16}$$

2.2. Boundary conditions

In the present study, no slip boundary condition was allocated for the non-porous wall surfaces, where both velocity components were set to zero at that boundary (*i.e.* $u = v = 0$). This boundary condition is located at the outer walls of the twisted heat exchanger. A constant heat flux $\left(100 \ W / m^2\right)$ was applied to the inner pipe of the heat exchanger, and a uniform water velocity inlet and a constant inlet temperature were assigned at the annulus inlet. At the exit of the twisted heat exchanger, the pressure was specified as atmospheric pressure at $\left(P = 0\right)$. The thermal boundary conditions for the water flow in the annular region of the double pipe heat exchanger are defined as follows:
At the inlet of the annulus, $x = 0$:

$$u = u_{in}, \tag{2.17}$$

$$v = 0, \tag{2.18}$$

$$T = T_{in}. \tag{2.19}$$

At the outlet of the annulus, $x = L$:

$$P = P_{atm},\tag{2.20}$$

$$\frac{\partial \varnothing}{\partial x} = 0.\tag{2.21}$$

At the walls of the outer square twisted duct:

$$U = v = 0,\tag{2.22}$$

$$q = 0.\tag{2.23}$$

At the walls of the inner circular pipe:

$$U = v = 0,\tag{2.24}$$

$$q = q''.\tag{2.25}$$

3. Numerical solution

The software package, ANSYS-Fluent v.16.2, which was used in this study has been accurately examined and utilized to solve problems of forced and free-convection flow systems. Thus, the present numerical study was carried out using a computational fluid dynamics (CFD) code with the aid of ANSYS-Fluent v.16.2 solver in which a constant velocity inlet field is imposed as an inlet condition. In the numerical solution, equations $(2.5$ to $2.8)$ were discretized based on a semi-implicit scheme. The control volume technique with second order accuracy was used to solve numerically Navier-Stokes equations. The SIMPLEC algorithm was utilized to solve the continuity equation with the velocity domain and calculate the pressure value. The convergence criteria for all the dependent variables are fixed as *0.00001*. The relaxation factors used in the simulation work are Energy *1.0*, Density *1.0*, Body force *1.0*, Pressure *0.3*, and Momentum *0.7*.

4. Grid type and grid independent solution

In the primary stage, the effect of the grid nodes number on the results accuracy was analysed. Consequently, it was noticed that an adequate degree of accuracy could be reached using (*306000* nodes) for the smooth heat exchanger model and (*733348* nodes) for the twisted heat exchanger model, as illustrated in Fig.3.
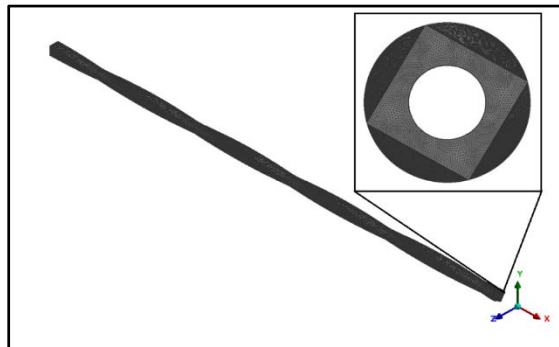
Fig.3. Computational domain meshing of the problem for triangular rib geometry.

The change in the velocity components, distribution of the wall heat fluxes, vorticity, and other factors did not exceed *0.1%* with an additional increase in the nodes number. In the present study, the enhanced wall treatment model was selected for the near-wall modeling process because it depends on a fine near-wall mesh, which is appropriate for resolving the viscous sub-layer. Local grid refinement was applied in the boundary layers. Adaptive grid refinement was also used in the preliminary computations. A grid independent solution was evaluated by comparing the friction factors and Nusselt numbers of various grid levels. The comparison revealed that the deviations in the findings between those at cell numbers of *532578* from those at cell numbers of *856547* were within *1.23%* for the Nusselt number and *1.01%* for the friction factor.

4. Results and discussion

The study of mixed convection heat transfer features for water flow in a twisted double-pipe heat exchanger system is of particular interest, since such heat transfer systems are usually employed in engineering arrangements. In the present work, numerical analysis was employed as the basis for a comparative examination of the fluid flow and heat transfer features of a more complex, three-dimensional swirl flow inside the annular region of the heat exchanger, constructed with a twisted outer duct and an inner circular pipe, when recirculation and separation of the water flows can play a significant role in the heat exchanger's operation. Although the length of the heat exchanger was fixed, the heat exchanger's geometry was varied in order to understand any resulting effects. The effect of the Reynolds number was also studied. The improvement in the velocity and temperature contours inside the annular region due to the twisted outer duct at the same $\mathrm{Re}=60$ and $\mathrm{Ra}=5\times10^8$ are shown in Figs 4 and 5, respectively. Here, each of the contours represents a velocity and temperature distribution in the cross section in the inlet $(x/L=0)$, the outlet $(x/L=1.0)$, and in the three middle sections of the double pipe heat exchanger for different twisted angles. In addition, the flow stabilizes rapidly and is already at the inlet of the annular region (x/L) for all twist angles in the boundary layers and takes on a classical laminar flow form. As the flow accelerates towards the center of the pipe at $(x/L=0.4)$, the maximum of the plume contours of the temperature begins to divert from the vertical direction to the inclined direction of the twisted angle of the outer duct. This outcome is due to an increase in the convective force of the fluid because of the swirl water flow being influenced by the twisted path of the outer square duct. This will lead to an increase in the circulated fluid around the heated inner pipe. The maximum temperature increased with an increase in the twist angle.

The effect of increasing the twist angle of the outer duct on the velocity contours is presented in Fig.5. For the case of the smooth heat exchanger with $(\theta=0)$, the velocity contour of the annular channel appears more uniformly. In addition, there are closed layers of fluids that have zero velocity near the wall due to the non-slip wall boundary condition but with an increase toward the center inside the annular region. However, when there is an increase in the twist angle, the results show that the maximum water velocity will rotate about the inner pipe until it becomes concentred in the upper zone of the annular region. In addition, the results reveal that the maximum velocity increases when there is an increase in the twist angle.

The temperature distribution of water flow in six position sections and for four (a/d) ratios of a twisted square annulus $a=19\ mm$ is presented in Fig.6. A conformity in the temperature distribution can be noticed. In addition, higher temperature quantities correspond with the higher level of heat transfer when utilizing ribs along the heated wall. Also, it can be seen that the heat transfer decreases as it moves to the end of the channel. This is also the case not only for the weak natural convection, but also when the aerodynamics does not practically change but has a significant contribution. Temperature counters of water flow in six position sections and for four (a/d) ratios of a twisted square annulus $d=12.6\ mm$ are shown in Fig.7. The distribution is periodic, and the corresponding maximum and minimum numbers exactly repeat the alternating nature of the location of the heated triangular ribs on the heated wall.
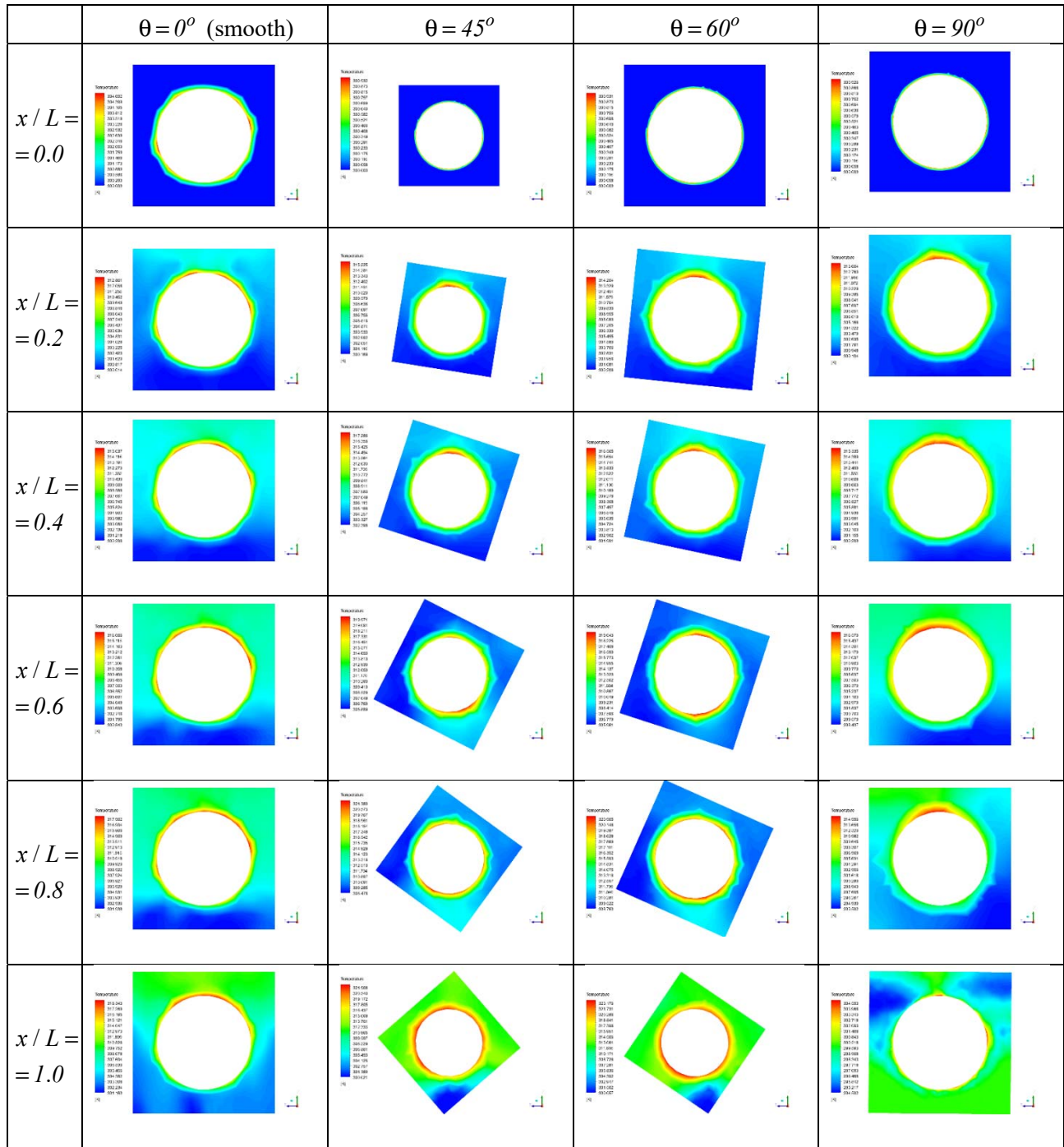
	θ = 0° (smooth)	θ = 45°	θ = 60°	θ = 90°
x / L = = 0.0				
x / L = = 0.2				
x / L = = 0.4				
x / L = = 0.6				
x / L = = 0.8				
x / L = = 1.0				

Fig.4. Temperature counters of water flow in six position sections and four twist angles of a twisted square annular where $a / d = 1.5$, $\text{Re} = 60$ and $\text{Ra} = 5 \times 10^8$.

	θ = 0° (smooth)	θ = 45°	θ = 60°	θ = 90°
x / L = *= 0.0*				
x / L = *= 0.2*				
x / L = *= 0.4*				
x / L = *= 0.6*				
x / L = *= 0.8*				
x / L = *= 1.0*				
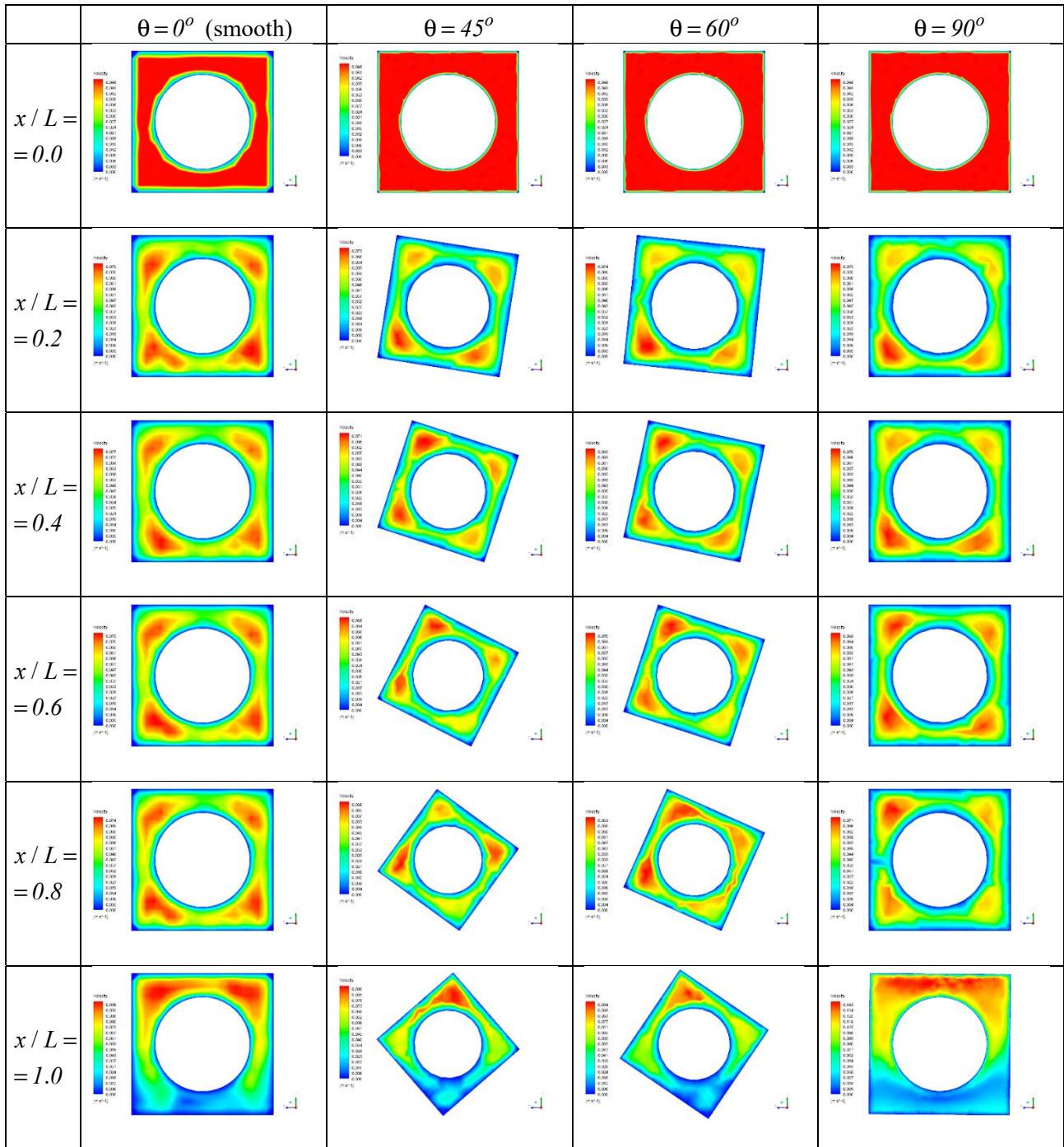
Fig.5. Velocity counters of water flow in six position sections and four twist angles of a twisted square annular, where *a / d = 1.5*, Re = *60* and Ra = *5×10⁸*.
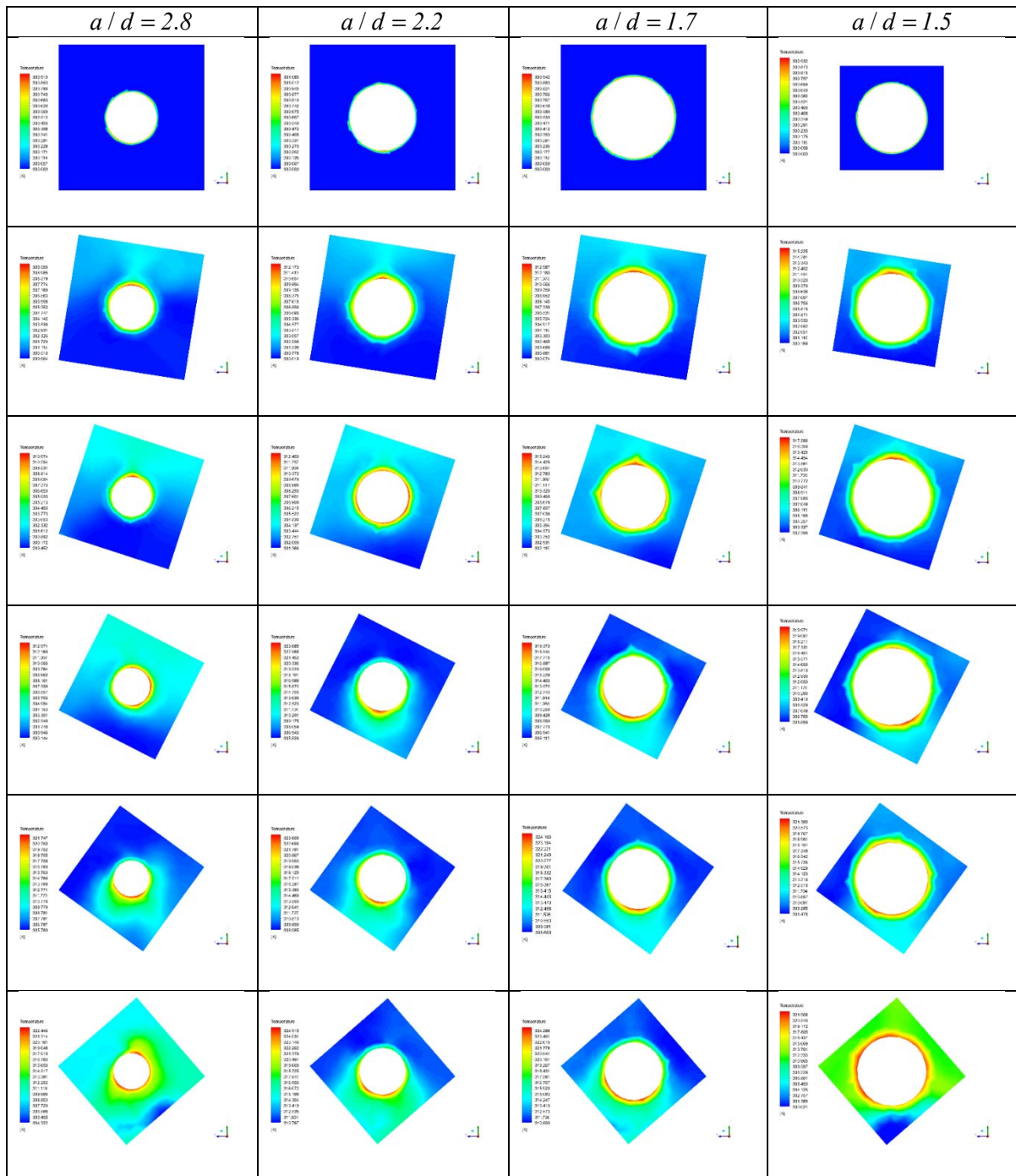
Fig.6. Temperature counters of water flow in six position sections and for four (a/d) ratios of a twisted square annulus $a = 19\ mm$, $Re = 60$ and $Ra = 5 \times 10^8$.
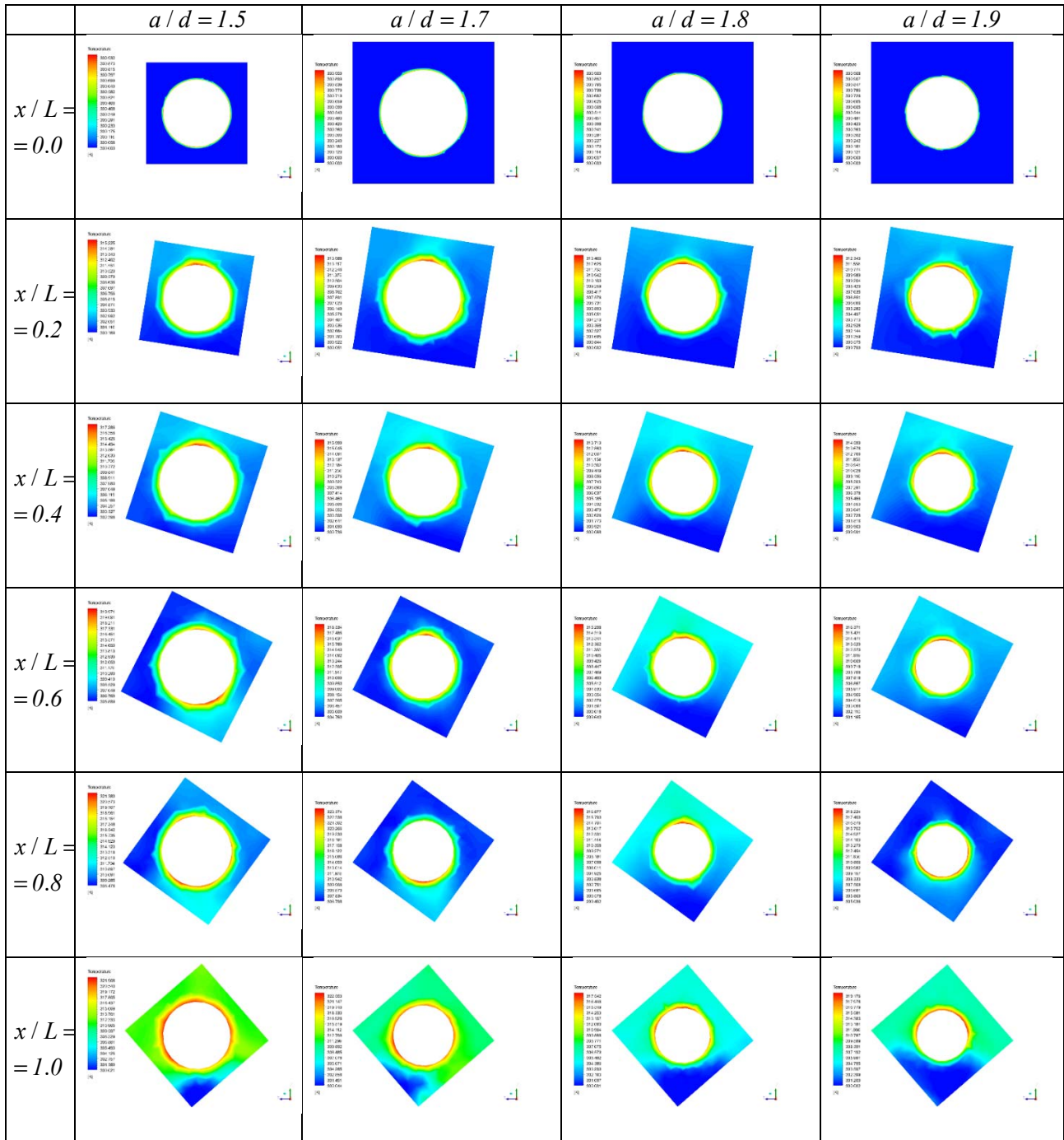
Fig.7. Temperature counters of water flow in six position sections and for four (a/d) ratio of a twisted square annulus $d = 12.6$ *mm*, $Re = 60$ and $Ra = 5 \times 10^8$.

The average values of the Nusselt number have an identical profile and continuous distribution. The numerical data for the different diameters of the inner pipe (d) of the twisted heat exchanger, and for various outer square sides (a), are plotted in Fig.8 and Fig.9, respectively. The results show that the average values of the Nusselt number increased with an increase in the Reynolds number and with a decrease in the inner pipe diameter. Moreover, it can be concluded that the maximum value of the Nusselt number is reached at the

minimum inner pipe diameter $(d = 6.6\ mm)$. The results confirm that the maximum Nu improved by about *30%* when utilizing a model of heat exchanger with d=6.6 instead of $d = 12.6$ mm at $\mathrm{Re} = 600$. However, the average Nusselt number increases with an increase in the outer dimension of the heat exchanger. Thus, the average Nusselt number increases by *25 %* when using a model of heat exchanger with $a = 25$ instead of $a = 19\ mm$ at $\mathrm{Re} = 600$.
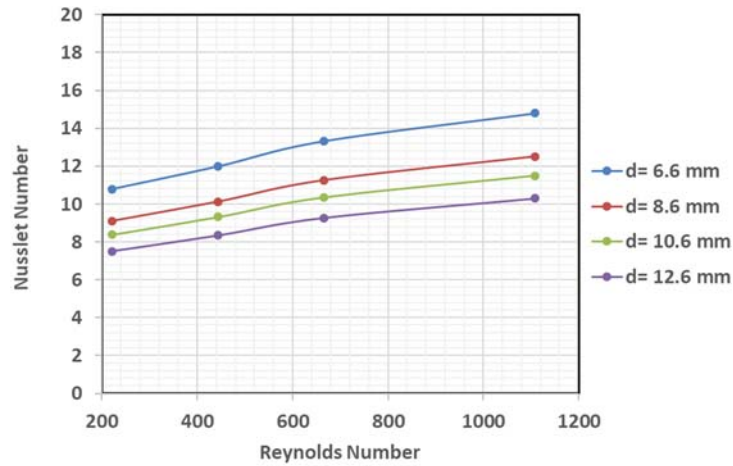
Fig.8. The relation between Reynolds and Nusselt number of air flow with (upstream) triangular ribs for various inner diameters.
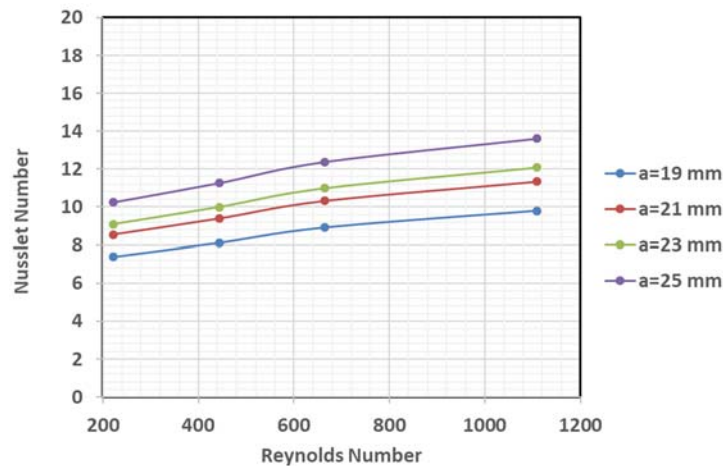
Fig.9. The relation between Reynolds and Nusselt number of air flow with (dowstream) triangular ribs for various outer diameters.

The behavior of the Nusselt numbers in respect of the angle of twist when there is a change in the Reynolds number is shown in Fig.10. The Nusselt numbers increase with an increase in the Reynolds number and with the angle of twist. The results show that the average Nusselt number increases by *47 %* when utilizing a heat exchanger with a twist angle of $\left(\theta = 90^o\right)$ instead of a twist angle of $\left(\theta = 0^o\right)$. This difference is due to an increase in the acceleration of the fluid flow in the twisted heat exchanger when compared with a conventional heat exchanger. Simultaneously, there is a desire to make the thermal system of ribs located far from the waste section more stable. These features of the variables behavior in the seperated heating mode should be taken into account when analyzing stepwise heat transfer systems.
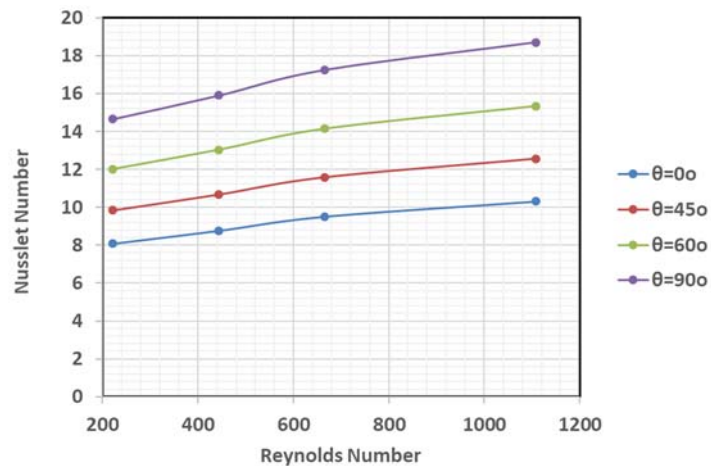
Fig.10. The relation between Reynolds and Nusselt number of air flow at constant Grashof numbers for various twist angles.
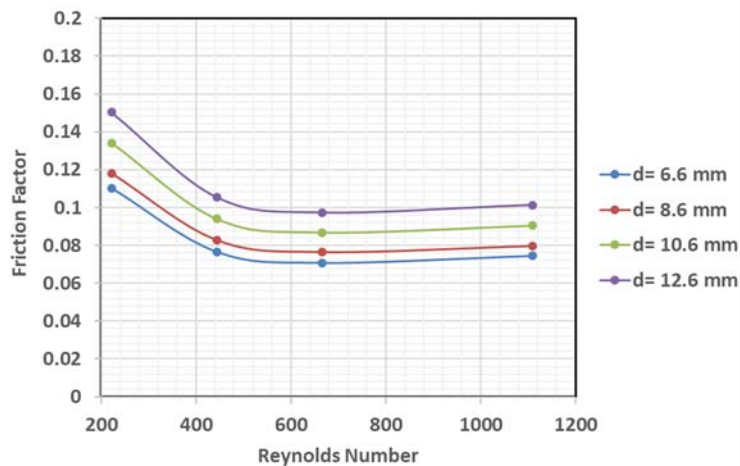
Fig.11. Effects of the Reynolds number on the friction factor of air flow with (upstream) triangular ribs for various inner diameters.

The effect of increasing the inner diameter together with varying the Reynolds number of water flow in the annular region on the friction factor is presented in Fig.11. The results show that the friction factor increases from *0.07* to *0.1* with an increase in the inner diameter of the heat exchanger from *6.6* to *12.6 mm*. The effect of increasing the outer dimension of the heat exchanger on the friction factor is presented in Fig.12. The results reveal that the friction factor increases with a decrease in the outer dimension (a). The friction factor increases from *0.06* to *0.08* when there is a decrease in the outer diameter from *25* to *19mm* at Re = *600*. The effect of increasing the angle of twist on the friction factor is plotted in Fig.13. The results show that the friction factor increases with an increase in the twist angle of the heat exchanger. The friction factor increases from *0.07* to *0.1* when there is an increase in the angle of twist from *0°* to *90°* at Re = *600*. However, in order to decide the best geometry parameters for the twisted heat exchanger, the thermal enhancement factor (TEF) as a function of the Reynolds number must be taken into account.
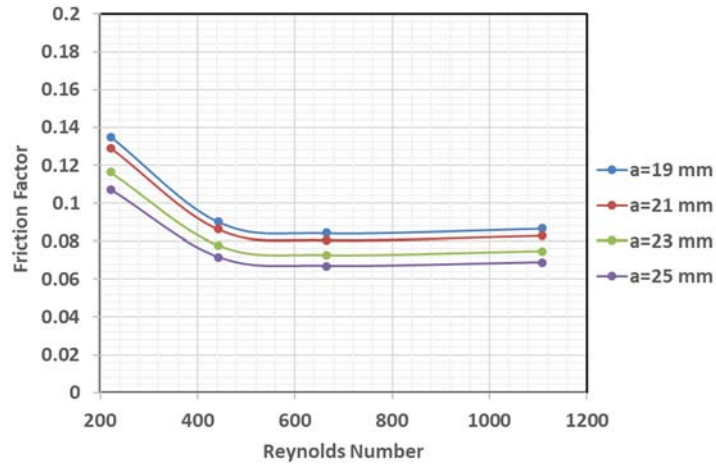
Fig.12. Effects of the Reynolds number on the friction factor of air flow with (downstream) triangular ribs for various outer diameters.
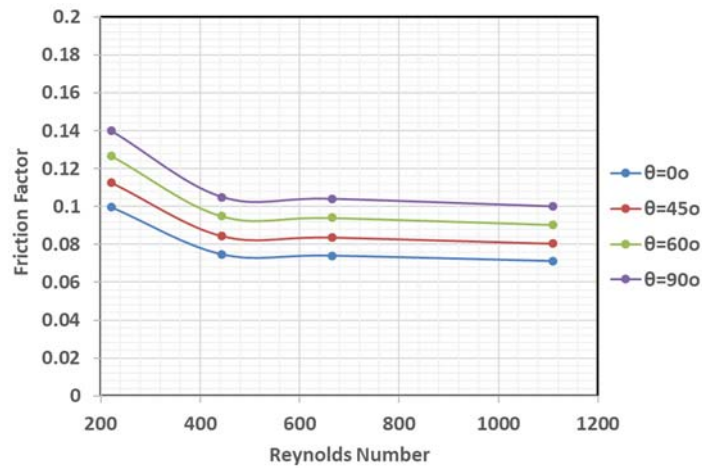
Fig.13. Effects of the Reynolds number on the friction factor of air flow at constant Grashof numbers for various twist angles.
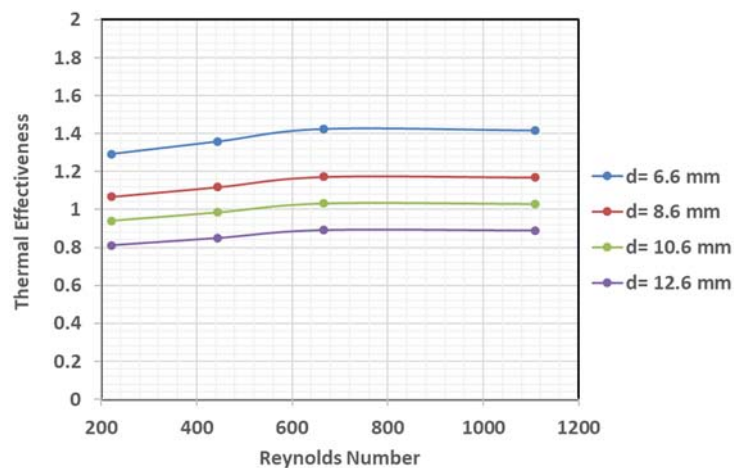
Fig.14. Variation of the thermal enhancement factor (TEF) with the Reynolds number for various inner diameters.
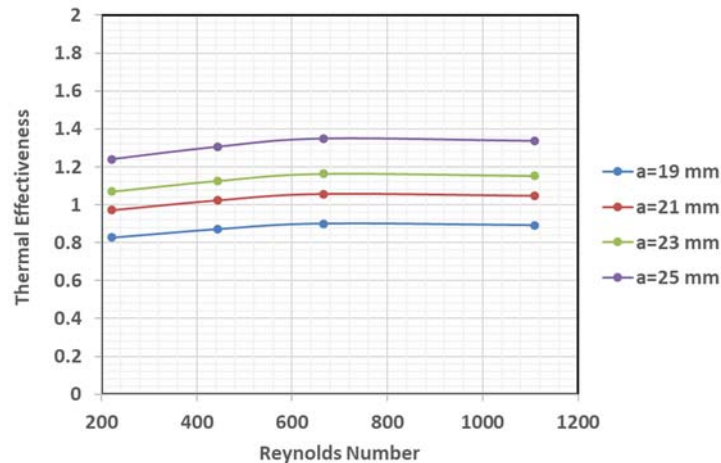
Fig.15. Variation of the thermal enhancement factor (TEF) with the Reynolds number for various outer diameters.
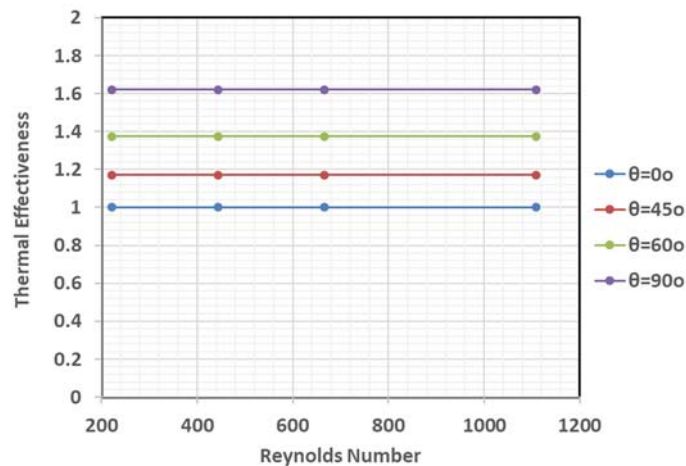
Fig.16. Variation of thermal enhancement factor (TEF) with the Reynolds number for various twist angles.

Figures 14, 15 and 16 plot the effect of the inner diameter, outer diameter and angle of twist, respectively, on the TEF. The results show that the maximum TEF is achieved with a lower inner diameter $(d = 6.6\ mm)$, a higher outer diameter $(a = 25\ mm)$, and at a higher twist angle $(\theta = 90^o)$.

5. Conclusion

The numerical studies of forced convection heat transfer in the laminar regime revealed a strong heterogeneity of the average Nusselt number and friction factor of water flow in the annular region between the inner circular cylinder and the outer square tube of the double pipe heat exchanger. This numerical calculation has been presented for various flows and heat transfer variables, such as the Richardson number Reynolds number, and Grashof number. The findings indicate that considerable changes in heat transfer rates from an individual twist angle depend on the twist angle, inner diameter and outer diameter. It has been established that the average Nusselt number for the heat exchanger is changed when the Reynolds number changes, as in the case of a classical flow in a laminar flow system. The results show that the average Nusselt number values increase with a decrease in the inner pipe diameter. The average Nusselt number increases

with an increase in the outer dimension of the heat exchanger. Finally, the Nusselt number increased with an increase in the Reynolds number and with the angle of twist.

Nomenclature

C_f – skin friction coefficient

C_p – specific heat for air, $[J.kg-1.K-1]$

f – friction factor

f_o – friction factor of smooth channel

H – channel height $[m]$

h – triangular rib height, $[m]$

k – thermal conductivity $[W/m.K]$

L – channel height $[m]$

Nu_o – Nusselt number of smooth channel

Nu_x – local Nusselt number

Nu – average Nusselt number

p – triangular rib pitch $[m]$

P – pressure $[Pa]$

Pr – Prandtl number

q – heat flux $\left[W/m^2\right]$

R – gas constant $[J/mol.K]$

T – temperature $[K]$

T_{in} – Inlet temperatures in x directions $[m/s]$

u – axial velocity $[m/s]$

U, V – dimensionless velocity components in x, y directions

u, v – velocity components in x, y directions $[m/s]$

u_{in} – Inlet velocity in x directions $[m/s]$

v – transverse velocity $[m/s]$

w – triangular rib width, $[m]$

x, y – Cartesian coordinates

X, Y – Cartesian dimensionless coordinates

Greek symbols

μ – dynamic viscosity $[Pa\ s]$

θ – dimensionless temperature

ρ – density $\left[kg/m^2\right]$

v – kinematics viscosity $\left[m^2 / s \right]$

Δ – difference

References

[1]   Van der Vyver S. and Meyer J.P. (1997): *Heat transfer augmentation in the annulus of a tube inside a twisted square tube.*– R&D Journal, vol.13, No.3, pp.77–82.

[2]   Timité B., Jarrahi M., Castelain C. and Peerhossaini H. (2009): *Pulsating flow for mixing intensification in a twisted curved pipe.*– Journal of Fluids Engineering, vol.131, Article number 121104, p.10.

[3]   Bhattacharyya S., Chattopadhyay H., Pal T.K. and Roy A. (2016): *Numerical investigation of thermohydraulic performance in elliptical twisted duct heat exchanger.*– In: Mandal D.K., Syan C.S. (eds) CAD/CAM, Robotics and Factories of the Future. Lecture Notes in Mechanical Engineering. Springer, New Delhi. https://doi.org/10.1007/978-81-322-2740-3_81.

[4]   Castelain C., Mokrani A., Le Guer Y. and Peerhossaini H. (2001): *Experimental study of chaotic advection regime in a twisted duct flow.*– Eur. J. Mech. part.B: Fluids, vol.20, pp.205-232.

[5]   Eiamsa-ard S. and Changcharoen W. (2015): *Flow structure and heat transfer in a square duct fitted with dual/quadruple twisted-tapes: influence of tape configuration.*– Journal of Mechanical Science and Technology, vol.29, No.8, pp.3501-3518.

[6]   Patil S. V. and Vijay Babu P.V. (2014): *Laminar heat transfer augmentation through a square duct and circular tube fitted with twisted tapes.*– Experimental Heat Transfer, vol.27, pp.124-143.

[7]   Promvonge P., Suwannapan Supattarachai, Monsak Pimsarn and Chinaruk Thianpong (2014): *Experimental study on heat transfer in square duct with combined twisted-tape and winglet vortex generators.*– Int. Commun. Heat Mass Transf., vol.59, pp.158-165.

[8]   Promvonge P. (2015): *Thermal performance in square-duct heat exchanger with quadruple V-finned twisted tapes.*– Applied Thermal Engineering, vol.91, pp.298-307.

[9]   Rashidi S., Akbarzadeh M., KarimiN. And Masoodi R. (2018): *Combined effects of nanofluid and transverse twisted-baffles on the flow structures, heat transfer and irreversibilities inside a square duct-A numerical study.*– Applied Thermal Engineering, vol.130, pp.135-148.

[10] Yang, S., Zhang Li and Hong Xu (2011): *Experimental study on convective heat transfer and flow resistance characteristics of water flow in twisted elliptical tubes.*– Applied Thermal Engineering, vol.31, pp.2981-2991.

[11] Zhang L., Sheng Yang and Hong Xu (2012): *Experimental study on condensation heat transfer characteristics of steam on horizontal twisted elliptical tubes.*– Applied Energy, vol.97, pp.881-887.

[12] Jehhef K.A., Badawy F.A. and Hussein A.A. (2021): *Thermal performance enhancement of the mixed convection between two parallel plates by using triangular ribs.*– International Journal of Applied Mechanics and Engineering, vol.26, No.2, pp.11-30.